Stretching Helical Semiflexible Polymers

Vikas Varshney and Gustavo A. Carri*

The Maurice Morton Institute of Polymer Science, The University of Akron, Akron, Ohio 44325-3909

Received October 9, 2004; Revised Manuscript Received November 14, 2004

ABSTRACT: We study the elastic behavior of a helical semiflexible polymer under extension. The polymer is described with a coarse-grained model recently developed by us (V. Varshney, et al. *Macromolecules* **2004**, *37*, 8794) where the chain is modeled using the freely rotating chain model and each bead can be in one of two possible conformations, helix or coil, depending on the value of its torsion. In this study, we extend the original model to include the effect of external mechanical forces and solve it using a Monte Carlo simulation approach based on the Wang−Landau sampling scheme. We found that the application of a mechanical force first increases the helix-to-coil transition temperature and then decreases it. This nonmonotonic behavior is a consequence of a change in the nature of the helix−coil transition which becomes a helix−extended coil transition for strong forces. We also found that the force−elongation curve at constant temperature displays three different behaviors depending on the temperature of the system. At temperatures below or slightly above the helix−coil transition temperature the force−elongation curve shows one or two coexistence regions, respectively. In these regions, helical sequences and random coil domains coexist while the strength of the force and temperature determine the fraction of the polymer adopting each conformation. At high temperatures, our model recovers the elastic behavior of a random coil. We also present a quantitative comparison of our simulation results with the theoretical ones obtained by Buhot and Halperin, and very good agreement is found. A qualitative comparison with experimental data for Xanthan is also presented.

Introduction

It is a well-established fact that novel conformations in biological, as well as synthetic, macromolecules can be induced by the application of a mechanical force.[1] These conformations are different from the ones generated by more traditional methods such as chemical or thermal denaturation and are inaccessible to conventional methods of measurement like X-ray crystallography and NMR.[2] Thus, the application of a mechanical force and the measurement of the resulting strain, generally referred to as single molecule force spectroscopy (SMFS), provide a novel perspective on the structure of macromolecules and the determinants of their mechanical stability. Some of the macromolecules studied using SMFS include biological molecules such as RNA[3] and DNA,[4] polysaccharides such as dextran[5] and xanthan,[6] the muscle protein Titin,[7] the extracellular matrix protein Tenascin,[8] and others, as well as synthetic polymers such as poly(ethylene glycol),[9] poly(vinyl alcohol),[10] and poly(L-gultamic acid).[11]

The abundant experimental results obtained for biomacromolecules using SMFS pose an enormous challenge for the theoretical community, which has to develop analytical models to capture the observed experimental behaviors. Developing such models has proven to be a formidable task due to the high complexity of the aforementioned biological macromolecules. However, theoretical investigations in some very specific cases have been done.[12] Indeed, these systems are highly complex due to many reasons such as molecular-level structural properties, which include chemical structure and tacticity, and energetic considerations such as electrostatic interactions, hydrogen bonding capabilities, preferred dihedral angles, van der Waals interactions, etc. The complexity of these systems at the molecular level results in a hierarchy of structures, proteins (with their primary, secondary, and tertiary structures) being one of the most common examples. However, there are biopolymers, called homopolypeptides, which are probably the simplest systems to study and have been modeled theoretically by various research groups. These macromolecules are capable of forming α-helices and undergo the helix−coil transition as a function of temperature in the absence of external forces. This behavior is commonly described using traditional theories of helix−coil transition.[13] The force−elongation behavior of polypeptides has also been the subject of intense research in recent years. For example, Pincus and collaborators[14] have studied the elastic behavior of homopolypeptides under stretching and Halperin and co-workers[15] have addressed the extension of helicogenic polypeptides and rod−coil block copolymers. It has been found that the application of a mechanical force on these polypeptides at temperatures just above their melting temperatures, T^*, results in a force−elongation behavior that displays two plateaus associated with the coexistence of helical and coil domains. For low to moderate values of the applied force, the first plateau corresponds to the helix-formation induced by chain extension, which is accompanied by the corresponding loss in configurational entropy. On the other hand, for large forces, the plateau corresponds to the extension-induced melting of the helical structure which occurs when the end-to-end distance exceeds the length of the helix. Kessler and Rabin[16] have also studied the force−elongation behavior of a helical spring and found that, under some conditions, when the force is increased, the end-to-end distance displays upward jumps (stretching instabilities). They showed that each jump was associated with the disappearance of helical turns and that the number of jumps depends on the length of the spring.

The subject of stretching biomacromolecules has also been investigated through various complementary com-

* Author to whom correspondence should be addressed. E-mail: gac@uakron.edu.

10.1021/ma047910b CCC: $30.25
Published on Web 12/30/2004

putational approaches such as molecular dynamics and Monte Carlo simulations. The advantages of these methods are clear: they provide a molecular-level understanding of the conformations, configurations, and interactions of the macromolecule. For example, molecular dynamics simulations have been used to study the deformation of DNA[17] and the mechanical extension of polypeptides such as polyalanine.[18] In addition, Monte Carlo simulations have also been performed to study the force−elongation behavior of macromolecules using both coarse-grained and all-atom descriptions of the chain. Specifically, de Pablo and collaborators have studied reversible mechanical unfolding of protein oligomers through the Wang−Landau algorithm by constructing the potential of mean force associated with the unfolding behavior.[19] Afterward, they calculated the density of states in the framework of an expanded ensemble, which they refer as the EXEDOS method, to analyze the force−elongation behavior. The Wang−Landau scheme mentioned above permits fast and self-consistent calculation of the density of states associated with arbitrary processes. Finally, the equilibrium conformations of synthetic oligomers as a function of extension have also been investigated using first-principle ab initio methods.[20]

In a recent article, we have successfully implemented the Wang−Landau sampling scheme to study the helix−coil transition of a semiflexible polymer described by a coarse-grained minimal model.[21] In this article, we explore how a helical semiflexible polymer described by our model responds when a mechanical force is applied to it. We restrict the discussion to the "quasi-static force" (in Buhot and Halperin's terminology),[15] where the rate of equilibration of the configurations of the chain is much faster than the rate of change of the force. Following the above line of thought, we compute the force−elongation behavior of helical semiflexible polymers using Monte Carlo simulations and rationalize the equilibrium properties of the chain in the different regimes in terms of its configurational, conformational, and thermodynamic properties.

This article is organized as follows. In the next section, we describe our simulation protocol. First, we provide a brief description of our model. Afterward, we describe the simulation methodology. In the next section, we present our results and rationalize the dependences of various equilibrium properties on temperature and applied force. Moreover, we compare our simulation results with the results obtained in ref 15 for the extension of polypeptides. Finally, we conclude the present article by summarizing the most important findings of our work and with the appropriate acknowledgments.

Model And Simulation Protocol

A. The Model. The details of our model for helical semiflexible polymers have been published elsewhere.[21] In this section, we present a brief description of the model and extend it to study the effect of mechanical forces on the equilibrium properties of the chain. In our minimal model, a polypeptide molecule is mapped onto the freely rotating chain model where each amino acid residue is represented by a bead. The bond length, equal to 1.53 in arbitrary units, and bond angle, equal to 109.3°, between consecutive beads are kept constant throughout the course of the simulation study.

Considering the fact that polypeptides undergo the helix−coil transition upon changes of temperature, all the models that describe this transition should capture its most important characteristic: the cooperativity of the transition. This cooperativity emerges from the formation of a hydrogen bond between the pair of residues i and $i + 4$ which, in turn, constrain the spatial positions and orientations of residues $i + 1$, $i + 2$, and $i + 3$. We capture this cooperative nature of the helix−coil transition using a criterion based on the concept of "torsion" of a curve, which is a well-defined mathematical quantity. Explicitly, this concept is employed as a criterion to determine the conformational state (helix or coil) of each bead. The torsion of a curve parametrized by the vectorial field $\mathbf{r}(x)$, which could be visualized as a continuous representation of the polymer chain, is defined as follows

$$\chi(x) = \frac{(\mathbf{r}'(x),\mathbf{r}''(x),\mathbf{r}'''(x))}{|[\mathbf{r}'(x),\mathbf{r}''(x)]|^2} \tag{1}$$

where x is the arc of length parameter that can take any value in the interval $[0,L]$, L being the total contour length of the chain, $\mathbf{r}'(x)$, $\mathbf{r}''(x)$, and $\mathbf{r}'''(x)$ are the first-, second-, and third-order derivatives of $\mathbf{r}(x)$, respectively. The square brackets and parenthesis indicate vectorial and scalar triple product (i.e., $(\mathbf{A},\mathbf{B},\mathbf{C}) = \mathbf{A}\cdot(\mathbf{B} \times \mathbf{C})$), respectively. This definition of torsion is also valid for the discrete representation of the polymer chain; the only difference is that the derivatives of the field must be approximated using finite differences. For example, the first-order derivative of the field on the ith bead is

$$\mathbf{r}'(i) \approx \frac{\mathbf{r}(i+1) - \mathrm{r}(i-1)}{2l_{\mathrm{K}}} \tag{2}$$

where l_{K} is the bond (Kuhn) length and $\mathbf{r}(i)$ is the position of the ith bead. Similar expressions are also available for the second- and third-order derivatives.[22]

It is well known that a perfect helical curve has a fixed torsion.[23] If we try to superimpose the beads that represent the polymer chain onto this imaginary helical curve, these beads should also have a constant value of torsion. We call this value *the torsion of the perfect helix*, χ_{Helix}. The value χ_{Helix} was chosen to be 0.87 and corresponds to two consecutive dihedral angles of +90°. Consequently, we defined the following criterion: "a bead has a helical conformation if the value of its torsion differs from the torsion of the perfect helix, χ_{Helix}, by less than a certain cutoff value, χ_{Cutoff}". The cutoff, χ_{Cutoff}, is set to 0.001. This value ensures that there is only *one* configuration of the chain that corresponds to the "perfect helix". If this criterion is satisfied, then this helical bead carries a negative enthalpy, called C, which stabilizes the helical conformation; otherwise, the bead is in the random-coil state, which is the reference state of the system. The enthalpic parameter C is related to the standard parameter s of helix−coil transition theory[13] as follows

$$s = \exp(-\Delta A/k_{\mathrm{B}}T) \quad \text{where } \Delta A = C - T\Delta S \tag{3}$$

It provides the enthalpic contribution that arises from the formation of a hydrogen bond and is assumed to be constant in our model. Furthermore, ΔS is the decrease in the entropy of the residue incorporated into a helical sequence due to the formation of a new hydrogen bond. The origin of ΔS in our model arises from the freely rotating chain (FRC) model and the constraints in the dihedral angles. Both parameters C and ΔS are negative in eq 3.

B. Modelling Force. The application of force on the polymer chain is shown in Figure 1. In the model, one end of the polymer chain is fixed at the origin while the polymer chain is stretched by applying force at its other end. We set the force to point in the positive x direction and investigate the equilibrium conformations of the polymer by plotting the average end-to-end distance and other properties for various temperatures and forces.

C. Simulation Methodology. In this article, the Wang−Landau sampling algorithm has been implemented to estimate the density of states (DOS) of the system.[24] Due to its fast and self-consistent nature, this algorithm has been successfully employed to study various phenomena in many fields. The

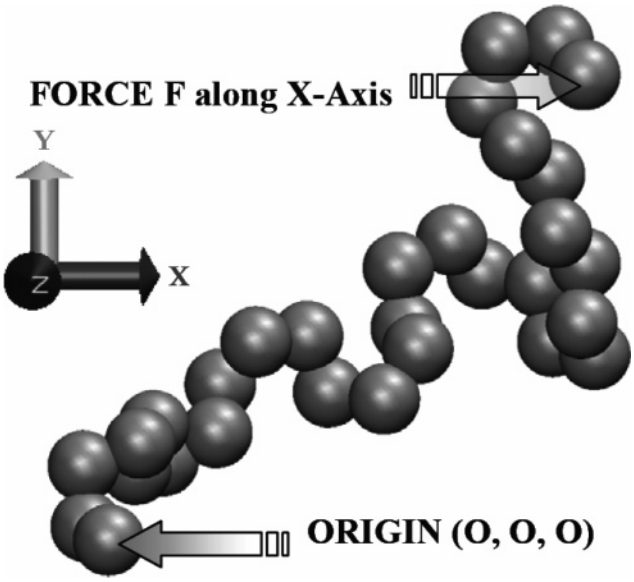

Figure 1. Graphical representation of the application of force on a helical semiflexible polymer chain at one of its ends fixing the other end at the origin.

algorithm generates a random walk in energy space with a probability proportional to the reciprocal of the DOS, $g(E)$, and leads to a flat energy histogram. Analogous to the multicanonical algorithm,[25] this algorithm has the advantage of escaping local energy minima and exploring the free energy landscape efficiently which, in turn, leads to an accurate estimate of the DOS. Another striking feature of this algorithm is the fact that it is independent of temperature, which makes it very useful to study a broad variety of systems.

Let us consider an arbitrary configuration of the polymer chain which is generated through the course of the simulation. This configuration has two relevant parameters necessary for the implementation of the Wang−Landau sampling algorithm; they are the number of beads in the helical state, N_s, and the projection of the end-to-end vector onto the direction of the applied mechanical force, R_x. If we imagine that this configuration of the chain is somehow generated by applying some force, F, acting along the positive x direction, then we can write the energy for this configuration as follows

$$E = CN_s - |F|R_x \tag{4}$$

which implies that, first, the contribution of the force term is zero when $F = 0$ or $R_x = 0$ and the energy depends on N_s only; second, if $N_s = 0$ for any configuration, then the energy depends only on R_x. Observe that the units of force are degrees Kelvin times reciprocal length.

It is clear from eq 4 that, at constant force, the energy, E, of a configuration depends on N_s and R_x and can be written as $E = E(N_s,R_x)$. Hence, the density of states (DOS) for this energy, $g(E)$, is also a function of N_s and R_x and can be denoted as $g(N_s,R_x)$. Furthermore, provided that the force acts along positive x direction, we can safely assume that $g(N_s,R_x) = g(N_s, -R_x)$ due to the symmetric nature of the system with respect to the $y-z$ plane. For this reason, we only consider the modulus of R_x when estimating the DOS. However, we use both, $g(N_s,R_x)$ and $g(N_s, -R_x)$ separately when calculating various equilibrium properties, as we explain below.

The dependence of the DOS on N_s and R_x is illustrated more clearly in Figure 2. In this schematic, the vertical axis corresponds to number of beads in the helical state, N_s, which increases in steps, while the horizontal axis is continuous because R_x is a real variable. So, we discretize this horizontal axis by binning it in intervals of width equal to 0.5 in the same arbitrary units of the bond length. Therefore, any configuration generated by the simulation is allocated in one of the squares

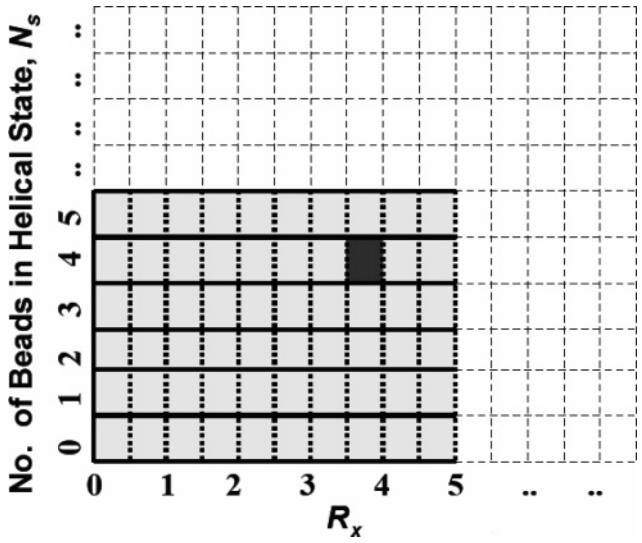

Figure 2. Schematic graph of the bin distribution with respect to the number of beads in the helical state, N_s, and the absolute value of the projection of the end-to-end vector along the x axis, R_x.

shown in Figure 2. For example, if the configuration of the chain has four helical beads and $R_x = 3.57$, then this configuration would be assigned to the shaded bin in Figure 2.

Let us review the Wang−Landau algorithm briefly. At the beginning of the simulation, the density of states, $g(N_s,R_x)$, which is unknown a priori, is initialized to 1 for all possible values of N_s and R_x. Furthermore, the corresponding histogram is set to 0. The random walk is then started by changing the configuration of the polymer using pivot moves. The transition probability for switching the polymer configuration from $\{N_{si},R_{xi}\}$ to $\{N_{sf},R_{xf}\}$ is given by

$$\text{Prob}(N_{si}, R_{xi} \rightarrow N_{sf}, R_{xf}) = \min\left(1, \frac{g(N_{si},R_{xi})}{g(N_{sf},R_{xf})}\right) \tag{5}$$

Each time a move is accepted, the DOS of the new configuration is updated by multiplying the existing value of the DOS by a modification factor, f, i.e., $g(N_s,R_x) \rightarrow g(N_s,R_x) \times f$. However, if the move is rejected, then the DOS of the old configuration is updated. This modification allows the random walk to explore the energy space corresponding to various values of N_s and R_x quickly and efficiently. The starting value of f is taken to be $e^1(=2.71828)$, as recommended by Wang and Landau. After a move is completed, the corresponding histogram, $H(N_s,R_x)$, is updated along with the modification of the DOS. Once the histogram is "flat" within some tolerance, the value of f is modified using Wang and Landau's recommendation as follows $f_{\text{new}} = \sqrt{f_{\text{old}}}$. At this point, the histogram is reset to 0 and the above procedure is started again with the updated modification factor. This procedure is repeated until the value of f is very close to 1. We stopped our simulations when $f - 1$ became smaller than 10^{-7}.

Once the DOS is known, various ensemble averages of interest can be calculated using standard formulas of statistical mechanics. For example, the mathematical expressions for the canonical partition function, Helmholtz free energy, internal energy, entropy, and heat capacity are

$$Z(T,C,F) = \sum_{N_s,R_x} g(N_s,R_x)(e^{-\beta(CN_s-FR_x)} + e^{-\beta(CN_s+FR_x)}) \tag{6}$$

$$A(T,C,F) = -T \ln(\sum_{N_s,R_x} g(N_s,R_x)(e^{-\beta(CN_s-FR_x)} + e^{-\beta(CN_s+FR_x)})) \tag{7}$$

$$U(T,C,F) = \langle E \rangle_T = \frac{\sum_{N_s,R_x} g(N_s,R_x)((CN_s - FR_x)e^{-\beta(CN_s-FR_x)} + (CN_s + FR_x)e^{-\beta(CN_s+FR_x)})}{\sum_{N_s,R_x} g(N_s,R_x)(e^{-\beta(CN_s-FR_x)} + e^{-\beta(CN_s+FR_x)})} \quad (8)$$

$$S(T,C,F) = \frac{U(T,C,F) - A(T,C,F)}{T} \quad (9)$$

$$Cv(T,C,F) = \frac{\langle E^2 \rangle_T - \langle E \rangle_T^2}{T^2} \quad (10)$$

where $A(T,C,F)$, $U(T,C,F)$, $S(T,C,F)$, and $Cv(T,C,F)$ are in units of Boltzmann constant, k_B. Apart from these thermodynamic quantities, the ensemble average of any other quantity of interest, $\langle AA \rangle$, can also be calculated as follows

$$\langle AA(T,C,F) \rangle = \frac{\sum_{N_s,R_x} g(N_s,R_x)(AA(N_s,R_x)e^{-\beta(CN_s-FR_x)} + AA(N_s,-R_x)e^{-\beta(CN_s+FR_x)})}{\sum_{N_s,R_x} g(N_s,R_x)(e^{-\beta(CN_s-FR_x)} + e^{-\beta(CN_s+FR_x)})} \quad (11)$$

Results and Discussion

A. Constant Force Scenario. Let us start by presenting our results for the case of a thirty-bead chain under a *constant* mechanical force. Figure 3 shows the mean square end-to-end distance, $\langle R^2 \rangle$, as a function of temperature for forces with increasing strengths. At $F = 0$, the polymer chain undergoes the traditional helix−coil transition discussed in our previous article in detail.[21] In this case, the equilibrium conformation at low temperature corresponds to an all-helix conformation while, at high temperatures, the chain adopts the random-coil conformation. As the strength of the force increases, some new features start to appear. First of all, it is clear from the figure that at any temperature, $\langle R^2 \rangle_{\text{Force}\neq 0} \geq \langle R^2 \rangle_{\text{Force}=0}$. This result is the direct consequence of the fact that the force is stretching the polymer chain in its direction and, hence, increasing its mean square dimensions. Second, it is also clear from the same figure that, for weak forces, the chain dimension decreases with increasing temperature, while it increases for strong forces. We refer to the decrease of $\langle R^2 \rangle$ with increasing temperature as the "helix−coil" transition, whereas we call the increase of $\langle R^2 \rangle$ with increasing temperature the "helix−extended coil" or "helix−stretch" transition. Also observe that, at sufficiently high strengths of the force, no transition is observed in the investigated temperature range. This is a result of the high strength of the applied force that destroys the helical structure of the chain even at low temperatures, where the chain displays an *extended-coil* conformation.

In addition, Figure 3 also highlights another interesting feature concerning the behavior of transition temperature as a function of force. Observe that the transition temperature, T^*, first increases and then begins to decrease with increasing strength of the applied force. This trend in T^* is more clearly observed in Figure 4 where the position of the peak of the heat capacity, which corresponds to T^*, is plotted as a function of the applied force. Apart from other features which were discussed before, a maximum in T^* is

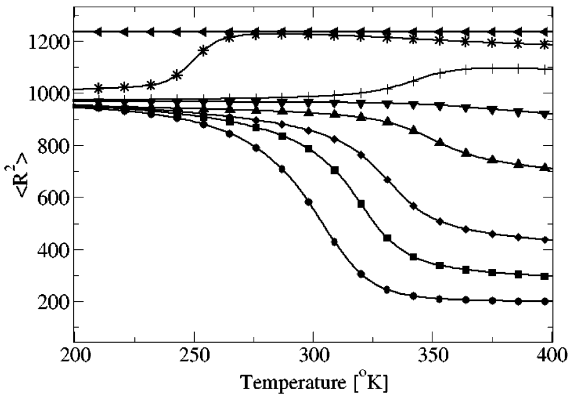

Figure 3. Plot of the mean square end-to-end distance, $\langle R^2 \rangle$, as a function of temperature for different values of the applied force. The parameters are: (●) $F = 0$, (■) $F = 100$, (◆) $F = 200$, (▲) $F = 500$, (▼) $F = 1000$, (+) $F = 2000$, (∗) $F = 4000$, and (left pointing solid triangle) $F = 8000$.

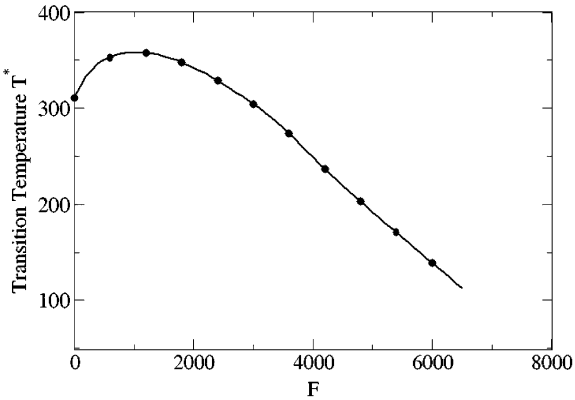

Figure 4. Plot of the transition temperature, T^*, as a function of the applied force.

observed for values of the force close to 1000. Figure 3 also shows a change in the behavior of $\langle R^2 \rangle$ for values of the force close to 1000. This crossover indicates a change in the character of the transition from the "helix−coil" to the "helix−extended coil" transition. We rationalize the behavior of T^* and the consequent change in the nature of the transition below.

When the system undergoes the "helix-to-coil" transition for low strengths of the force, this transition is essentially temperature-driven, i.e., temperature is the governing factor for breaking the helical structure. So, weak forces basically favor the "formation of the helical conformation" and, hence, shift the transition temperature to higher temperatures. The stabilization of the helical structure by the application of a weak force can be rationalized using basic concepts of statistical mechanics as follows. When the force is applied, the entropy of the chain is reduced and the probability of visiting states that correspond to stretched configurations of the chain increases. Among these states are those that include helical sequences; thus, stretching the chain increases the probability of visiting states with helical domains. Consequently, the formation of helical sequences is facilitated by the application of a weak force. On the other hand, the "helix-to-extended coil" transition which happens for high strengths of the force is force-driven, i.e., the force is the primary factor for the disintegration of the helical structure. During this transition, the melting of the helical domains is a consequence of the *overstretching* (with respect to the length of the helix) of the chain. The stronger the force,

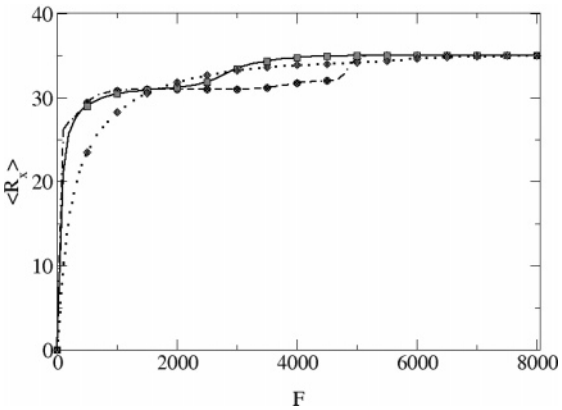

Figure 5. Plot of the mean end-to-end distance, $\langle R_x \rangle$, as a function of the applied force for different temperatures. The parameters are: (●) $T = 200$ K, (■) $T = 315$ K, and (◆) $T = 500$ K.

the lower the temperature needed to destroy the helical structure. Consequently, the transition temperature decreases with increasing force. This decrease is simple to understand using basic thermodynamic concepts. Indeed, the application of a *strong* stretching force decreases the probability of forming long helical sequences. Thus, most of the helical domains are *short* in this regime, i.e., they contain few helical beads, and consequently, are less thermodynamically stable. This results in a lower transition temperature. Finally, the transition from one kind of behavior to the other one occurs for strengths of the force near the maximum in Figure 4.

B. Constant-Temperature Scenario. We now proceed to study how different properties of the chain depend on the applied force when the temperature is kept constant. It has been stated in the literature that, during the formation and disintegration of the helical structure due to the application of force, two coexisting *phases* occur in a certain temperature window.[15] One of those phases is made of helical sequences while the other one is made of random coils. This temperature window is governed by factors such as the elastic free energy of the stretched coil, A_{el}, the Zimm−Bragg parameter, s, and the ratio $\gamma = R_{helical}/R_{stretch}$, where $R_{helical}$ and $R_{stretch}$ correspond to the end-to-end distance of the perfect helix and fully stretched polymer, respectively. The lower limit of this temperature window is T^* where the helix-coil transition takes place in absence of force, i.e., where $s = 0$, while the upper limit is determined by T_c, which is defined as the temperature where free energy A_{el} is equal to free energy of helix A_h.[15] T_c is approximately equal to 400 K for our model. Furthermore, at higher temperatures, no coexisting regions are observed while, at lower temperatures, there is only one coexisting region corresponding to the transformation of helical domains into extended-coil structures due to the application of force. Therefore, in this part of our study, we explore three temperatures corresponding to three different regimes, i.e., $T = 200$ K ($T < T^*$), $T = 315$ K ($T^* < T < T_c$), and $T = 500$ K ($T > T_c$).

Figure 5 shows the mean end-to-end distance, $\langle R_x \rangle$, as a function of the force for the temperatures mentioned above. $\langle R_y \rangle$ and $\langle R_z \rangle$ are equal to 0 for all values of temperature and force due to the symmetry of the problem. It can easily be seen from Figure 5 that, irrespective of the temperature, $\langle R_x \rangle$ is always 0 in the absence of force, as expected. As soon as force starts acting on the chain, the configurations of the chain shift toward positive values of $\langle R_x \rangle$, as can be observed in the figure. At low temperatures ($T = 200$ K), Figure 5 predicts an initial steep increase in $\langle R_x \rangle$ for low values of force followed by a plateau and an additional increase for higher values of force before the final plateau is reached. The initial increase in $\langle R_x \rangle$ should not be considered as a coexistence of helical and coil domains. Indeed, this increase simply reflects the alignment of the helical structure along the direction of the applied force. However, the second steep increase in $\langle R_x \rangle$, which occurs when $F \approx 5000$, is indeed a coexistence region due to the breaking of the helical structure. At high temperatures, $T = 500$ K, there is no coexistence of helical and coils domains as expected because the helical sequences have been melted. Here, the initial increase of $\langle R_x \rangle$ followed by a plateau region simply reflect the elastic nature of the random coil conformation of the chain at low values of force followed by the limited chain extensibility for stronger forces. Like in the low-temperature case, intermediate temperatures ($T = 315$ K) show two steep increases in $\langle R_x \rangle$ as a function of force. One occurs when $F \approx 200$, while the second one happens when $F \approx 3000$. Interestingly, unlike in the low-temperature scenario, here both increases in $\langle R_x \rangle$ correspond to coexistence of helical and coil domains. The first coexistence region occurs for weak forces and corresponds to the formation of helical structure from coil domains, while the other coexistence region corresponds to the transformation of helical sequences into extended coils.

To make our study more balanced and objective, we now proceed to compare the force−elongation curve predicted by our model, Figure 5, with experimental data obtained for native Xanthan.[6] Xanthan is an extracellular bacterial polysaccharide whose primary structure is known. Moreover, native Xanthan forms an ordered helical secondary structure stabilized by noncovalent bonds in solution. Upon an increase in temperature, Xanthan undergoes a temperature-induced order−disorder transition into a disordered single-strand state. Figure 5a of ref 6 shows two force−elongation curves of native Xanthan. This figure shows a monotonic increase in force followed by a relative sharp transition to a plateau. Upon further elongation of the molecule, the force starts to increase again until failure occurs. Observe that this force−elongation behavior is in good qualitative agreement with the force−elongation behavior predicted by our model and shown in Figure 5. In addition, it is interesting to observe that another polysaccharide called Dextran also shows this kind of force−elongation behavior.[5] In this case, the macromolecule undergoes a transition between two conformations with different *segmental elasticities*.

The different initial slopes of $\langle R_x \rangle$ for low and intermediate temperatures can be better understood by studying the mean square end-to-end distance, $\langle R^2 \rangle$, which we plot in Figure 6. This figure clearly shows that, irrespective of the strength of the force, $\langle R^2 \rangle$ is never 0. Furthermore, it is clear from the figure that at low temperatures ($T = 200$ K) there is no initial increase in $\langle R^2 \rangle$ for low values of force. This directly supports our previous argument that the initial steep increase in $\langle R_x \rangle$ is simply due to the alignment of the helical structure. However, at 315 K, one can clearly observe an increase in $\langle R^2 \rangle$, similar to the one in $\langle R_x \rangle$ seen in Figure 5, for

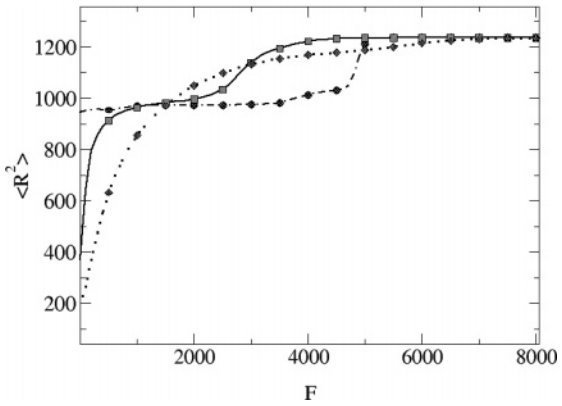

Figure 6. Plot of the mean square end-to-end distance, $\langle R^2 \rangle$, as a function of the applied force for different temperatures. The parameters are: (●) $T = 200$ K, (■) $T = 315$ K, and (◆) $T = 500$ K.

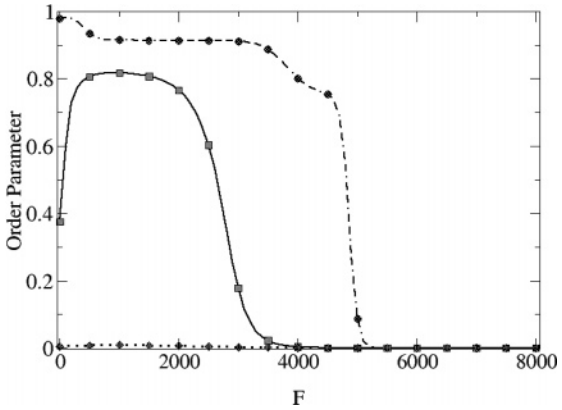

Figure 7. Plot of the order parameter (fraction of beads in the helical state) as a function of the applied force for different temperatures. The parameters are: (●) $T = 200$ K, (■) $T = 315$ K, and (◆) $T = 500$ K.

low values of the force. This indicates that, as the force increases, an increasing number of beads in the coil conformation become part of the existing helical sequences. Another important feature of Figures 5 and 6 is the fact that the force required to break the helical structure decreases with increasing temperature (second coexistence region). The breaking of the helical structure is essentially a force-driven transition, so the higher the temperature is, the more it favors the melting of helical structures and the weaker the force needed for the transition to occur. The remaining features in Figure 6 are similar to the ones in Figure 5 and can be rationalized using similar arguments.

Figure 7 shows the fraction of helical beads (order parameter) as a function of force for three temperatures: 200, 315, and 500 K. At high temperatures, 500 K, no coexistence is observed; the order parameter always remains equal to 0 and reflects the extension of a random coil. Furthermore, it also corroborates that, at high temperatures, the helical conformation is not a feasible equilibrium structure, irrespective of the force that is acting on the chain. On the other hand, the figure does show a coexistence regime at low temperatures, 200 K, where the sharp decay in the order parameter for high values of force clearly reveals the disintegration of helical structures. Moreover, Figure 7 also confirms the formation and disintegration of helical structures as a function of force at intermediate temperatures, 315 K, as demonstrated by an initial increase in order

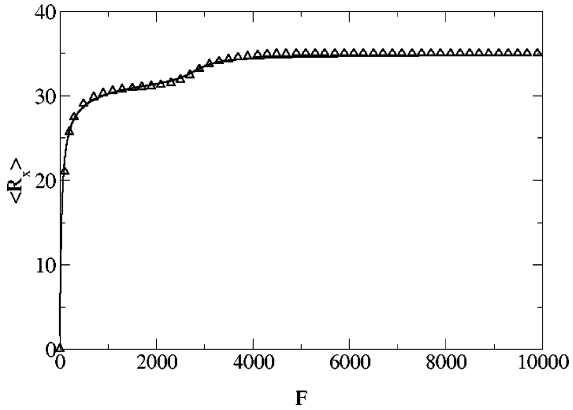

Figure 8. Force−elongation curve at 315 K. Continuous curve (Buhot and Halperin),[15] △ (this work).

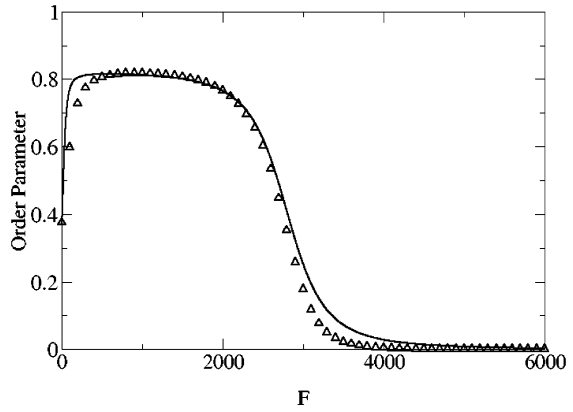

Figure 9. Order parameter as a function of the applied force at 315 K. Continuous curve (Buhot and Halperin after multiplication by 0.83),[15] △ (this work).

parameter followed by a sharp decrease to 0 at higher values of force. Therefore, it corroborates the existence of two coexisting regions of helical and coil domains.

Before finishing this section, we also compare our results with theoretical predictions made by Buhot and Halperin.[15] Figure 8 shows a quantitative comparison of our result for 315 K with the one obtained using the theory of Buhot and Halperin. The parameters of the theory are: $a = 5.073$, $\gamma = 0.961$, $n_h = 1134$, $P = 7.23$, $\sigma = 0.035$ and $\Delta S = -4.17$ (eq 3) where both a and P are expressed in the same arbitrary units used to measure the bond length in our simulation study and ΔS is in units of Boltzmann constant. We also remind the reader that the value of C in eq 3 is −1300 K. Observe that the quantitative agreement between the theoretical and simulation results is quite remarkable if we consider that the theory does not account for excluded volume interactions and uses the freely *jointed* chain model while the simulation does include excluded volume interactions and uses the freely *rotating* chain model. This suggests that the force−elongation behavior of the helical polymer does not depend *strongly* on the local details of the model, as long as the polymer adopts a helical structure. However, the differences between both models show up in other ensemble averages that depend more strongly on the local details of the model employed. Figure 9 shows the order parameter as a function of the applied force at 315 K using the values of the parameters of the theory given above. The results obtained from the theory of Buhot and Halperin had to be multiplied by an arbitrary prefactor equal to 0.83 to reach the agreement showed in the figure. After mul-

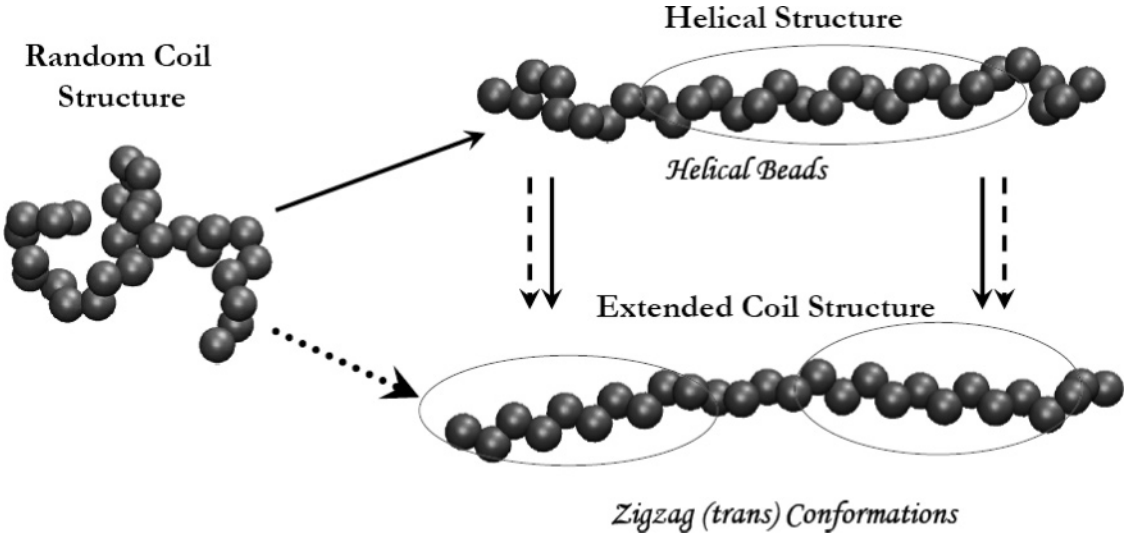

Figure 10. Schematic of various equilibrium conformations. The arrows represent an increase of the applied force. The dashed, line, and dotted arrows represent conformational changes at low temperatures ($T = 200$ K), intermediate temperatures ($T = 315$ K), and high temperatures ($T = 500$ K), respectively.

tiplication, the quantitative agreement between simulation and theory is again remarkable. The origin of the prefactor is the use of different models to describe the polymer chain, freely rotating chain against freely jointed chain, and the presence or absence of excluded volume interactions. However, it is surprising to see that these differences can be accounted for by a simple multiplicative prefactor in the order parameter.

Conclusions

In this article, we have studied the elastic properties of a single helical semiflexible polymer using Monte Carlo simulations. We found that, depending on the strength of the applied force, the average size of the chain can decrease or increase upon an increase in temperature. In the first case, the polymer undergoes the helix−coil transition, while in the second case, it undergoes a helix-extended coil transition. Moreover, we found that the application of force first increases the transition temperature and then decreases it. Physical arguments that rationalize this behavior were discussed in the text.

In the constant-temperature scenario, we found that, depending on the temperature of the system, three possible situations are encountered. If the temperature is below the transition temperature, then the initial application of force first orients the helical structure parallel to the force and then it starts melting the helical structure, which leads to a coexistence of helical sequences and random (extended) coil domains. A further increase of the applied force leads to a fully extended coil conformation. At temperatures slightly above the transition temperature, the elastic behavior of the chain presents two coexistence regions. First, for weak forces, the number of helical beads (order parameter) increases. In other words, the application of force stabilizes the helical conformation. This leads to a coexistence between helical and random coil domains. A further increase of the applied force starts melting the helical structures and leads to a coexistence between helical sequences and extended coil conformations. Finally, for very large forces, the polymer is in a fully extended conformation. At high temperatures, we found that the elastic behavior of a random coil is recovered by our model. These results are summarized in Figure 10. The tails of the arrows correspond to weak forces, while the heads of the arrows indicate strong forces.

Acknowledgment. This material is based upon work partially supported by the National Science Foundation under Grant No. CHE-0132278. Also, acknowledgment is made to the donors of the Petroleum Research Fund, administered by the American Chemical Society, for partial support of this research (PRF No. 37051-G7) and The Ohio Board of Regents, Action Fund (Grant No. R566).

References and Notes

(1) Poirier, M. G.; Nemani, A.; Gupta, P.; Eroglu, S.; Marko, J. F. *Phys. Rev. Lett*. **2001**, *86*, 360. Leger, J. F.; Romano, G.; Sarkar, A.; Robert, J.; Bourdieu, L.; Chatenay, D.; Marko, J. F. *Phys. Rev. Lett*. **1999**, *83*, 1066. Wang, M. D.; Yin, H.; Landick, R.; Gelles, J.; Block, S. M. *Biophys. J.* **1997**, *72*, 1335. Oberhauser, A. F.; Marszalek, P. E.; Erickson, H. P.; Fernandez, J. M. *Nature (London)* **1998**, *393*, 181. Smith, S. B.; Finzi, L.; Bustamante, C. *Science* **1992**, *258*, 1122.
(2) Fisher, T. E.; Marszalek, P. E.; Fernandez, J. M. *Nature Struct. Biol*. **2000**, *7*, 719.
(3) Harlepp, S.; Marchal, T.; Robert, J.; Leger, J.-F.; Xayaphoummine, A.; Isambert, H.; Chatenay, D. *Eur. Phys. J. E* **2003**, *12*, 605.
(4) Perkins, T. T.; Quake, S. R.; Smith, D. E.; Chu, S. *Science* **1994**, *264*, 822. Perkins, T. T.; Smith, D. E.; Chu, S. *Science* **1997**, *276*, 2016. Smith, S. B.; Cui, Y.; Bustamante, C. *Science* **1996**, *271*, 795.
(5) Rief, M.; Oesterhelt, F.; Heymann, B.; Gaub, H. E. *Science* **1997**, *275*, 1295.
(6) Li, H. B.; Rief, M.; Oesterhelt, F.; Gaub, H. E. *Adv. Mater.* **1998**, *10*, 316.
(7) Kellermayer, M. S. Z.; Smith, S. B.; Granzier, H. L.; Bustamante, C. *Science* **1997**, *276*, 1112. Rief, M.; Gautel, M.; Oesterhelt, F.; Fernandez, J. M.; Gaub, H. E. *Science* **1997**, *276*, 1109.
(8) Oberhauser, A. F.; Marszalek, P. E.; Erickson, H. P.; Fernandez, J. M. *Nature (London)* **1998**, *393*, 181.
(9) Oesterhelt, F.; Rief, M.; Gaub, H. E. *New J. Phys*. **1999**, *1*, 6.1.
(10) Li, H. B.; Zhang, W. K.; Xu, W. Q.; Zhang, X. *Macromolecules* **2000**, *33*, 465.
(11) Idiris, A.; Alam, M. T.; Ikai, A. *Protein Eng*. **2000**, *13*, 763.
(12) Reif, M.; Fernandez, J. M.; Gaub, H. E. *Phys. Rev. Lett*. **1998**, *81*, 4764.
(13) Poland, D.; Scheraga, H. A. *Theory of Helix-Coil Transition in Biopolymers*; Academic Press: New York, 1970.
(14) Tamashiro, M. N.; Pincus, P. *Phys. Rev. E* **2001**, *63*, 021909.

(15) Buhot, A.; Halperin, A. *Phys. Rev. Lett*. **2000**, *84*, 2160. Buhot, A.; Halperin, A. *Macromolecules* **2002**, *35*, 3238.
(16) Kessler, D. A.; Rabin, Y. *Phys. Rev. Lett*. **2003**, *90*, 024301.
(17) Olson, W. K.; Zhurkin, V. B. *Curr. Opin. Struct. Biol*. **2000**, *10*, 286.
(18) Masugata, K.; Ikai, A.; Okazaki, S. *Appl. Surf. Sci*. **2002**, *188*, 372.
(19) Rathore, N.; Yan, Q.; de Pablo, J. J. *J. Chem. Phys*. **2004**, *120*, 5781.
(20) Kreuzer, H. J.; Wang, R. L. C.; Grunze, M. *New J. Phys*. **1999**, *1*, 21.1.
(21) Varshney, V.; Dirama, T. E., Sen, T. Z.; Carri, G. A. *Macromolecules* **2004**, *37*, 8794.
(22) Abramowitz, M.; Stegun, I. A. *Handbook of Mathematical Functions with Formulas, Graphs and Mathematical Tables*; Dover Publications: New York, 1965.
(23) Budak, B. M.; Fomin, S. V. *Multiple Integrals, Field Theory and Series*; MIR Publishers: Moscow, 1973.
(24) Wang, F.; Landau, D. P. *Phys. Rev. Lett.* **2001**, *86*, 2050.
(25) Hansmann, U. H. E.; Okamoto, Y. *J. Comput. Chem*. **1993**, *14*, 1333. Okamoto Y.; Hansmann U. H. E., *J. Phys. Chem*. **1995**, *99*, 11276. Alves, N. A.; Hansmann, U. H. E. *J. Phys. Chem. B* **2003**, *107*, 10284. Kemp, J. P.; Chen, Z. Y. *Phys. Rev. Lett*. **1998**, *81*, 3880.

MA047910B